Role of the kinesin neck linker and catalytic core in microtubule-based motility

Ryan B. Case*, Sarah Rice*, Cynthia L. Hart†, Bernice Ly* and Ronald D. Vale*†

Kinesin motor proteins execute a variety of intracellular microtubule-based transport functions [1]. Kinesin motor domains contain a catalytic core, which is conserved throughout the kinesin superfamily, followed by a neck region, which is conserved within subfamilies and has been implicated in controlling the direction of motion along a microtubule [2,3]. Here, we have used mutational analysis to determine the functions of the catalytic core and the ~15 amino acid 'neck linker' (a sequence contained within the neck region) of human conventional kinesin. Replacement of the neck linker with a designed random coil resulted in a 200–500-fold decrease in microtubule velocity, although basal and microtubule-stimulated ATPase rates were within threefold of wild-type levels. The catalytic core of kinesin, without any additional kinesin sequence, displayed microtubule-stimulated ATPase activity, nucleotide-dependent microtubule binding, and very slow plus-end-directed motor activity. On the basis of these results, we propose that the catalytic core is sufficient for allosteric regulation of microtubule binding and ATPase activity and that the kinesin neck linker functions as a mechanical amplifier for motion. Given that the neck linker undergoes a nucleotide-dependent conformational change [4], this region might act in an analogous fashion to the myosin converter, which amplifies small conformational changes in the myosin catalytic core [5,6].

Addresses: *Departments of Pharmacology, Biochemistry and Biophysics and †Howard Hughes Medical Institute, 513 Parnassus Avenue, University of California, San Francisco, California 94143, USA.

Correspondence: Ronald D. Vale
E-mail: vale@phy.ucsf.edu

Received: **10 November 1999**
Accepted: **9 December 1999**

Published: **28 January 2000**

Current Biology 2000, 10:157–160

0960-9822/00/$ – see front matter

Results and discussion

In human conventional kinesin, the first ten residues following the conserved catalytic core (amino acids 323–332; Figure 1) are highly conserved among plus-end-directed kinesin motors [7]. To identify the role of these kinesin neck linker residues, we replaced them with ten non-native amino acids (ESGAKQGEKG, using the single-letter amino-acid code) designed to form a random coil termed ran10. We also prepared a partial mutation of the neck linker by changing the conserved residues Ile325, Lys326, and Asn327 to alanine (I325A/K326A/N327A). In addition, we prepared alanine substitutions of two conserved glycines in loop 13 of the catalytic core, Gly291 and

Figure 1

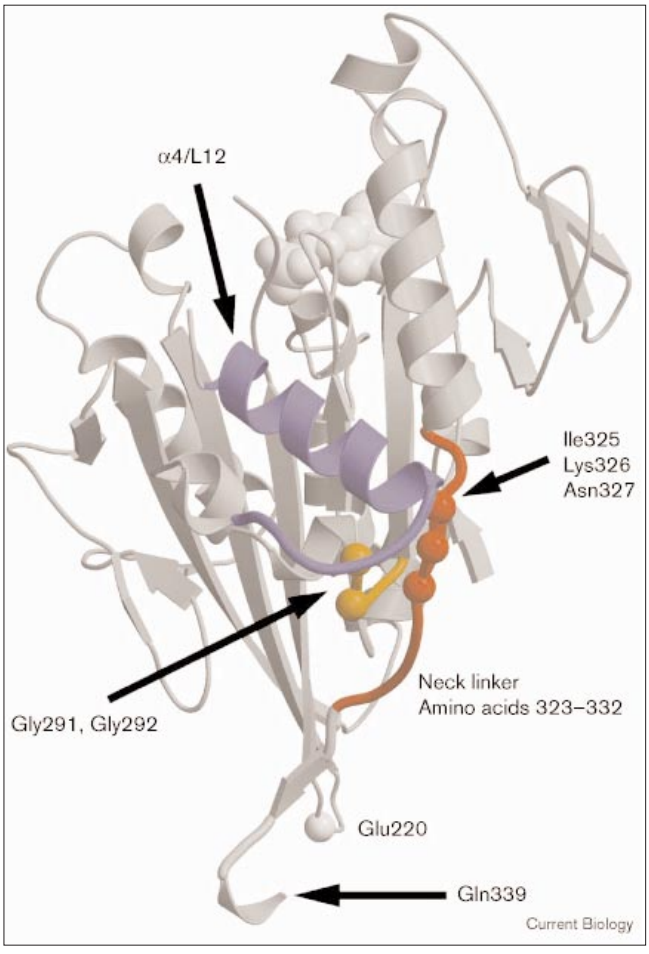

The catalytic core and neck linker of conventional kinesin (head B of the rat kinesin dimer crystal structure; PDB #3KIN [8]), as viewed from within the microtubule with the plus-end at the bottom. The catalytic core (amino acids 7–322; all numbers refer to human kinesin) is grey, α4 (the switch II helix) and loop 12 (L12; the primary microtubule-binding element) are purple, and amino acids 323–332 of the neck linker are red. The remainder of the neck linker (amino acids 333–336), the beginning of the neck coiled-coil domain (amino acids 337–339), and the bound ADP are also grey. Alpha carbons of some of the mutated residues are shown (Gly291 and Gly292 in loop 13 are orange; Ile325, Lys326, Asn327 in the neck linker are red). Gln339 is the junction point with GFP in K339–GFP. For energy-transfer experiments, tetramethylrhodamine was labeled at a single surface cysteine at position 220.

Figure 2

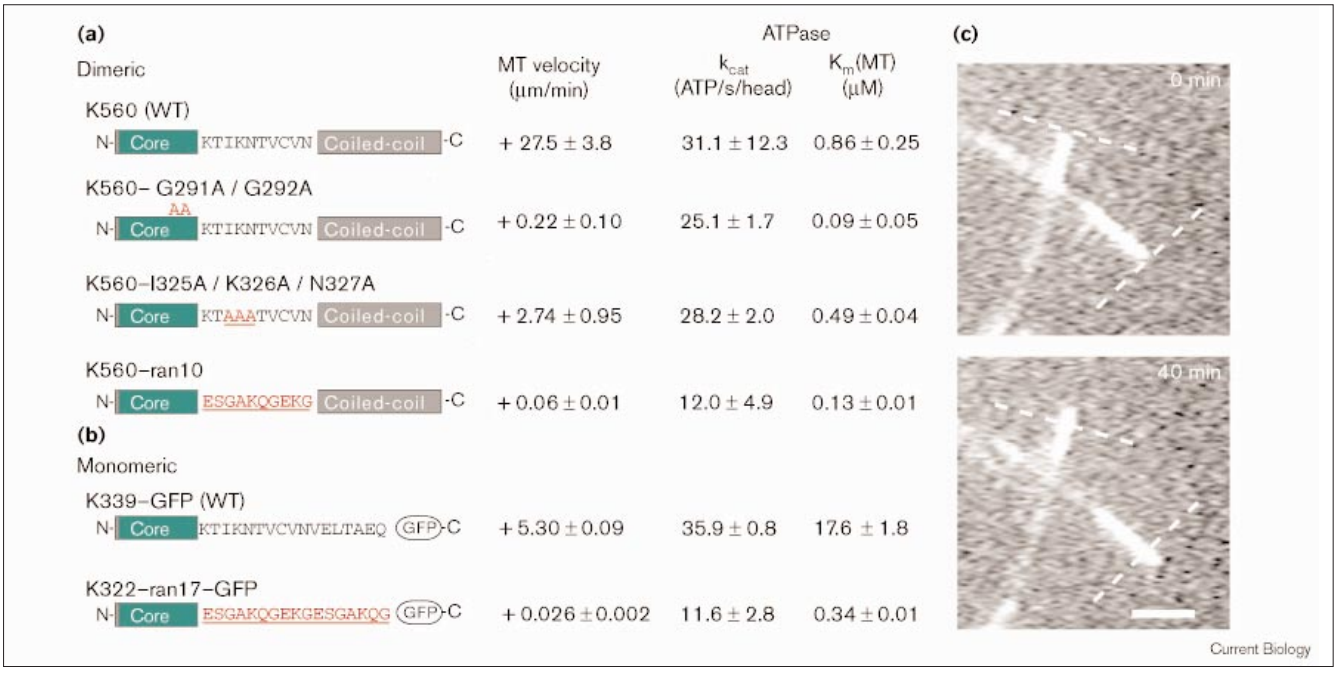

Mutagenesis of the kinesin neck linker in dimeric and monomeric kinesin motors. **(a,b)** Each construct is represented by a catalytic core (amino acids 1–322, green box) followed by neck linker residues (amino acids 323–332, K560; amino acids 323–339, K339–GFP) followed by (a) the neck coiled-coil domain, neck hinge (hinge 1) and first coiled-coil of the stalk domain (amino acids 333–560; grey box, K560 constructs) or (b) by a GFP moiety in the K339 constructs. Neck linker amino acids in black represent endogenous residues, whereas mutations are in red and are underlined. The glycine-to-alanine replacements, G291A and G292A, are represented by the letter A in red over their approximate location in the core. His_6 tags were present at the carboxyl terminus in all constructs, but are not shown. Wild-type values represent the mean and standard deviation (SD) from seven independent K560 and two K339–GFP preparations. For each mutant, microtubule velocities are mean ± SD of an average of 50 microtubule velocities (except K322–ran17–GFP, for which 22 velocities were measured) from at least two protein preparations; > 95% of the microtubules scored exhibited plus-end-directed motion. The ATPase values are mean ± SD from two curves plotted from two independent protein preparations. **(c)** Movement of microtubules by the single-headed construct K322–ran17–GFP. Two polarity marked microtubules brightly labeled at the minus end are shown for two time points; the initial positions of the microtubule minus-ends are marked with a dashed white line. The microtubules can be seen moving ~0.7 μm with their minus-ends leading, indicating a plus-end-directed motion of motors fixed on the coverslip. Given that motion occurred in perpendicular directions, the movement was caused by the motor proteins and is not due to stage drift. Scale bar, 2 μm.

Gly292 (G291A/G292A), the latter of which binds through hydrogen bonds to residue Asn327 of the neck linker [8]. These glycines, in addition to contacting the neck linker, might also be important for allowing motion within the catalytic core.

We assayed the above mutations in a dimeric kinesin construct (K560) for enzymatic and motile properties (Figure 2a). All mutations dramatically affected motor activity: microtubule gliding velocity in a multiple-motor assay was decreased by approximately 10-, 100-, and 500-fold in K560–I325A/K326A/N327A, K560–G291A/G292A, and K560–ran10, respectively. The maximal microtubule-stimulated ATPase rates (k_{cat}) of K560–I325A/K326A/N327A and K560–G291A/G292A were nearly the same as those of wild type, however. The k_{cat} of K560–ran10 was approximately one-third that of wild-type kinesin. These results indicate that these mutations of the neck linker and loop 13 do not severely disrupt the enzymatic cycle of the motor but rather mainly affect microtubule-based motility.

The small amount of motility produced by K560–ran10 suggested the possibility that the catalytic core alone might have motor activity. To test this hypothesis, we created a monomeric construct (K322–ran17–GFP; Figure 2b) that contains the catalytic core (amino acids 1–322) followed by 17 amino acids of the designed random coil (ESGAKQGEKGESGAKQG) linked to green fluorescence protein (GFP). The carboxy-terminal GFP was used to bind and orient the catalytic core onto the coverslip surface via surface-bound, anti-GFP antibodies, for motility assays as well as to perform spectroscopic measurements (see below). The 17 amino-acid linker served as a spacer so that association with the coverslip surface would not sterically inhibit microtubule binding. As a wild-type control, we prepared K339–GFP, which has

the 17 amino acids of the native neck linker between the catalytic core and GFP. K339–GFP exhibited plus-end-directed motility at a rate of 5.3 ± 0.8 μm/minute (Figure 2b), which was about fivefold slower than wild-type K560 but is similar to other single-headed kinesin constructs [9]. K322–ran17–GFP exhibited extremely slow plus-end-directed microtubule motility at 0.026 ± 0.002 μm/minute, which is 200-fold slower than K339–GFP but only half the speed of K560–ran10. To confirm that this slow motion was not due to stage drift, we measured the motion of perpendicularly oriented polarity-marked microtubules (Figure 2c).

In contrast to the substantial reduction in movement velocity, the microtubule-stimulated ATP turnover (k_{cat}) of K322–ran17–GFP was only threefold lower than that of wild type. Microtubules stimulated the ATPase activity of K322–ran17–GFP at much lower concentrations compared with K339–GFP (Figure 2a). The reason for the lower K_m (MT) is not clear, although it may be due to an increase in the number of ATP hydrolysis events per microtubule encounter. We also measured the basal ATPase rate in the absence of microtubules and found that steady-state turnover of K322–ran17–GFP (0.020 ± 0.005 ATP/s/head) was only slightly increased over K339–GFP (0.006 ± 0.001 ATP/s/head). A similar increase has been previously noted when kinesin was truncated into the neck linker region [10]. Thus, microtubules are still able to stimulate the ATPase activity of the catalytic core by ~600-fold. Because the only kinesin residues present in K322–ran17–GFP are those of the globular catalytic core, we conclude that the catalytic core itself is capable of producing a very small plus-end-directed motion on microtubules and has nearly normal microtubule-stimulated ATPase activity. These experiments also indicate that the endogenous neck linker functions to increase microtubule velocity by approximately 200-fold.

To determine how the neck linker influences microtubule binding, we measured microtubule affinity for both K322–ran17–GFP and K339–GFP under different nucleotide conditions. The equilibrium binding constants were similar in the presence of 1 mM AMPPNP, a non-hydrolyzable ATP analogue (K_d = 0.70 ± 0.07 μM and 0.88 ± 0.15 μM for K322–ran17–GFP and K339–GFP, respectively) or in the absence of nucleotide (apyrase treatment; K_d = 0.53 ± 0.15 μM and 0.44 ± 0.12 μM, respectively). In the presence of 1 mM ADP, however, K322–ran17–GFP exhibited a threefold higher microtubule affinity (6.9 ± 0.4 μM) than the corresponding wild-type protein (21.1 ± 3.4 μM). These results indicate that the neck linker specifically affects microtubule affinity during the ADP-bound state. As visualized by cryo-electron microscopy [4], the neck linker of the ADP-bound motor can adopt multiple conformations, one of which may be important for decreasing microtubule affinity.

Rice *et al.* [4] recently showed that the neck linker of microtubule-bound kinesin is mobile in the absence of nucleotide and then adopts a highly ordered state after binding AMPPNP. This ordering and extension of the neck linker towards the microtubule plus end was proposed to be the basis of plus-end-directed motility. The AMPPNP-induced transition can be measured by an increase in fluorescence resonance energy transfer (FRET) between the GFP (donor) at the end of neck linker in K339–GFP and tetramethylrhodamine (TMR; acceptor) introduced at a single engineered cysteine residue (Cys220; Figure 1) at the tip of the catalytic core [4]. We tested whether mutations in the neck linker affected this conformational change. Upon addition of 5 mM AMPPNP to nucleotide-free, microtubule-bound K339–GFP/TMR kinesin, a 22.5% increase in FRET efficiency was observed (see Materials and methods section). For K339–I325A/K326A/N327A–GFP/TMR and K322–ran17–GFP/TMR, however, little or no FRET increase was observed (< 3%). Thus, the neck linker mutants appear not to undergo the same AMPPNP-induced conformational change as wild-type kinesin.

In summary, we have shown that mutagenesis of the kinesin neck linker results in a 200–500-fold reduction of microtubule velocity with a less than threefold reduction of steady-state ATP turnover. In contrast, deletion of the neck coiled-coil [11] or neck hinge [12] regions results in, at most, an approximately fivefold reduction of microtubule velocity. Therefore, of the three neck regions, the ~15 amino-acid neck linker is the most crucial for motility. We have also shown that the kinesin catalytic core is capable of microtubule-regulated ATPase activity, nucleotide-dependent microtubule binding, and generating slow plus-end-directed motion. Interestingly, mutagenesis of the twelve conserved residues of the Ncd neck region also results in a slow plus-end motion on microtubules with normal microtubule-stimulated ATPase activity [13]. These findings suggest the possibility that throughout the kinesin superfamily, the catalytic core functions as an allosteric enzyme that interacts with microtubules and has a weak mechanical activity directed towards the microtubule plus-end. Class-conserved neck sequences might have evolved as mechanical amplifiers that confer unique motile properties to particular subfamilies of kinesin motors [7]. Some 'orphan' motors with highly divergent neck sequences [7], however, might operate primarily using the activity of the catalytic core alone.

We propose that the kinesin neck linker plays an equivalent role to the converter domain of myosin motors, which amplifies conformational changes in myosin's catalytic core and causes motion of the elongate lever arm helix [5,6]. The kinesin and myosin cores are structurally related [14], and the kinesin neck linker and the myosin converter are located in topologically equivalent locations

in the two motors. Moreover, both the unique neck region of carboxy-terminal kinesin motors [13,15,16] and the unique converter domain of myosin VI [6] appear to reverse directionality in these motor subfamilies. Further studies on the kinesin necks and myosin converters should provide additional insights into the motility mechanisms used by these two types of motor proteins.

Materials and methods

Cloning and protein preparation

Site-directed mutagenesis using Stratagene's QuikChange protocol (Stratagene Inc.) and subsequent subcloning of human kinesin K560 and K339-GFP constructs (all containing a carboxy-terminal His_6 tag) were performed as described [2]. The sequences of all constructs were verified. Bacteria (BL21) were freshly transformed with the expression vector pET17b, grown, induced with IPTG, lysed, and supernatants prepared as reported previously [2]. All proteins were applied to Ni-NTA resin (Qiagen Inc.) and eluted as described [2]. Further purification was performed by mono-Q or High Trap-Q chromatography (Pharmacia Inc.) in buffers containing 25 mM Pipes–KOH pH 6.8, 2 mM $MgCl_2$, 1 mM EGTA, using a NaCl salt gradient. K339–GFP and K560 eluted at 200 and 300 mM NaCl, respectively. Purity of the above proteins was in the range of 40–90%, with the majority of the contaminants representing degradation products. Protein concentration was measured as described [17]. Proteins were frozen (10% sucrose added) and stored in liquid nitrogen.

Functional assays

Kinesin proteins were assayed for microtubule-stimulated steady-state ATPase activity in 12 mM PIPES pH 6.8, 3 mM NaCl, 2 mM $MgCl_2$, 1 mM EGTA, 1 mM ATP, and 10 μM paclitaxel using a coupled-enzyme assay as previously described [17]. Multiple motor gliding assays were performed using rhodamine-labeled microtubules and fluorescence microscopy in flow cells as described [2]. All non-GFP-containing motors were adsorbed nonspecifically to the glass coverslip surface. For GFP-containing constructs, affinity-purified anti-GFP polyclonal antibodies were preadsorbed onto the coverslip and used to bind and orient the motor on the surface. For slow moving proteins (< 1 μm/min), polarity-marked, rhodamine-labeled microtubules were used to ensure that all motion was unidirectional, and the illumination was shuttered in order to reduce damage by free radicals. For K560–ran10 and K322–ran17–GFP, motility assays were run for up to 40 min in order to produce microtubule displacements longer than the visual distance threshold of ~0.2 μm. For measuring microtubule-binding affinity, K339–GFP or K322–ran17–GFP were incubated with 8–10 microtubule concentrations in 12 mM PIPES pH 6.8, 3 mM NaCl, 2 mM $MgCl_2$, 1 mM EGTA, 20 μM paclitaxel and 0.02 mg/ml BSA with 10 U/ml apyrase (no nucleotide), 1 mM AMPPMP (ATP-like state), or 1 mM ADP. Microtubules/kinesin–GFP were centrifuged ($100{,}000 \times g$) for 5 min, resuspended and depolymerized on ice in the above buffer without EGTA and paclitaxel and with 1 mM $CaCl_2$. The fraction of kinesin–GFP bound to microtubules was quantitated by fluorescence using a plate reader (SPECTRAFluor Plus, TECAN), and the binding constant was determined by fitting the data to a hyperbola.

FRET spectroscopy

All FRET measurements were performed using a previously described K339–GFP construct which has a single surface cysteine at position 220 (K339-GFP-E220C Cys Lite Mutant) [4]. For all wild-type and mutant preparations, this cysteine was labeled to ~1:1 molar ratio with tetramethylrhodamine as described [4] and purified from free dye by step elution on a mono-Q column with Q buffer (25 mM PIPES, 2 mM $MgCl_2$, 1 mM EGTA, 20 μM ATP, and 0.1 M TCEP-HCl) + 400 mM NaCl. The labeling stoichiometry was determined by measuring the TMR absorbance and protein concentration as described [4]. Steady-state fluorescence measurements were performed using a K2 spectrofluorimeter (ISS, Champaign-Urbana). Labeled kinesin, 10 μM microtubules, 10 U/ml Sigma Grade VII apyrase in Q buffer with 50 mM NaCl were placed in a cuvette for the nucleotide-free spectrum. MgAMPPNP (5 mM) was added to this sample for the AMPPNP spectrum. Measurements were made with ~1 μm, 0.5 μm, and 0.25 μm kinesin to ensure that energy transfer was not dilution-sensitive due to inner filter effects or reabsorption of donor emission. The energy-transfer efficiency was calculated by donor quenching estimated as $E = 1-(Fl_{DA}/Fl_{DO})$ where Fl_{DO} and Fl_{DA} are the donor fluorescence in the absence and presence of the acceptor, respectively [4].

Acknowledgements

We thank Roger Cooke, Robert Fletterick and Elena Sablin for helpful discussions.

References

1. Goldstein LSB, Philp AV: **The road less traveled: emerging principles of kinesin motor utilization.** *Annu Rev Cell Dev Biol* 1999, **15:**141-183.
2. Case RB, Pierce DW, Hom-Booher N, Hart CL, Vale RD: **The directional preference of kinesin motors is specified by an element outside of the motor catalytic domain.** *Cell* 1997, **90:**959-966.
3. Henningsen U, Schliwa M: **Reversal in the direction of movement of a molecular motor.** *Nature* 1997, **389:**93-96.
4. Rice S, Lin AW, Safer D, Hart CL, Naber N, Carragher BO, *et al.*: **A structural change in the kinesin motor protein that drives motility.** *Nature* 1999, **402:**778-784.
5. Houdusse A, Kalabokis VN, Himmel D, Szent-Gyorgyi AG, Cohen C: **Atomic structure of scallop myosin subfragment S1 complexed with MgADP: a novel conformation of the myosin head.** *Cell* 1999, **97:**459-470.
6. Wells AL, Lin AW, Chen LQ, Safer D, Cain SM, Hasson T, *et al.*: **Myosin VI is an actin-based motor that moves backwards.** *Nature* 1999, **401:**505-508.
7. Vale RD, Fletterick RJ: **The design plan of kinesin motors.** *Annu Rev Cell Dev Biol* 1997, **13:**745-777.
8. Kozielski F, Sack S, Marx A, Thormahlen M, Schonbrunn E, Biou V, *et al.*: **The crystal structure of dimeric kinesin and implications for microtubule-dependent motility.** *Cell* 1997, **91:**985-994.
9. Berliner E, Young EC, Anderson K, Mahtani H, Gelles J: **Failure of a single-headed kinesin to track parallel to microtubule protofilaments.** *Nature* 1995, **373:**718-721.
10. Jiang W, Stock M, Li X, Hackney D: **Influence of the kinesin neck domain on dimerization and ATPase kinetics.** *J Biol Chem* 1997, **272:**7626-7632.
11. Romberg L, Pierce DW, Vale RD: **Role of the kinesin neck region in processive microtubule-based motility.** *J Cell Biol* 1998, **140:**1407-1416.
12. Grummt M, Woehlke G, Henningsen U, Fuchs S, Schleicher M, Schliwa M: **Importance of a flexible hinge near the motor domain in kinesin-driven motility.** *EMBO J* 1998, **17:**5536-5542.
13. Sablin EP, Case RB, Dai SC, Hart CL, Ruby A, Vale RD, *et al.*: **Direction determination in the minus-end-directed kinesin motor ncd.** *Nature* 1998, **395:**813-816.
14. Kull FJ, Sablin EP, Lau R, Fletterick RJ, Vale RD: **Crystal structure of the kinesin motor domain reveals a structural similarity to myosin.** *Nature* 1996, **380:**550-555.
15. Hirose K, Lockhart A, Cross RA, Amos LA: **Three-dimensional cryoelectron microscopy of dimeric kinesin and ncd motor domains on microtubules.** *Proc Natl Acad Sci USA* 1996, **93:**9539-9544.
16. Endow SA, Waligora KW: **Determinants of kinesin motor polarity.** *Science* 1998, **281:**1200-1202.
17. Woehlke G, Ruby AK, Hart CL, Ly B, Hom-Booher N, Vale RD: **Microtubule interaction site of the kinesin motor.** *Cell* 1997, **90:**207-216.